MICRO-WRINKLED PD SURFACE FOR HYDROGEN SENSING AND SWITCHED DETECTION OF LOWER EXPLOSIVE LIMIT

Greco, F.[1], Ventrelli, L.[1,2], Dario, P. [1,2] and Mattoli, V.[3]
[1] Center for MicroBioRobotics @SSSA, Istituto Italiano di Tecnologia, Viale Rinaldo Piaggio 34, 56025, Pontedera (PI), Italy, francesco.greco@iit.it, virgilio.mattoli@iit.it
[2] Biorobotics Institute Polo Sant'Anna Valdera, Scuola Superiore Sant'Anna, Viale Rinaldo Piaggio 34, 56025 Pontedera (PI), Italy

ABSTRACT

We report the development and test of a novel hydrogen sensor that shows a very peculiar response to hydrogen exposure, due to its micro-structured Palladium surface. The fabrication of the wrinkled Pd surface is obtained using an innovative, fast and cheap technique based on the deposition of a thin Pd film onto thermo-retractable polystyrene sheet that shrinks to 40% of its original size when heated. The buckling of Pd surface induced by shrinking of substrate produce nano and micro-wrinkles on the entire sensor surface. The obtained microstructured sensor surface is very stable also after repeated hydrogen sorption/desorption cycles. The hydrogen sensing mechanism is based on the transitory absorption of hydrogen atoms into the Pd layer, leading to reversible change of its electrical resistance. Interestingly, depending on hydrogen concentration the proposed sensor shows the concurrent effect of both the usually described behaviors of increase or decrease of resistance, related to different phenomena occurring upon hydrogen exposure and formation of palladium hydride. The study reports and discusses evidences for an activation threshold of hydrogen concentration in air switching the behavior of sensor performances from, e.g., poor negative to large positive sensitivity and from slow to fast detection.

INTRODUCTION

Due to the increasing interest in the use of hydrogen as a fuel, the development of reliable hydrogen sensors for the detection of H_2 gas leakages and for the continuous monitoring of its concentration in many different industrial environments is the object of intensive research. The use of hydrogen as a possible alternative and "green" resource is indeed limited by many safety issues related to storage and handling, raised by its flammability and explosiveness: the Lower Explosive Limit (LEL) of H_2 in air is 4%. Different sensing technologies have been proposed and exploited to provide hydrogen detection [1]; most of these rely on the selective interaction of the hydrogen with palladium (Pd) or palladium alloys, because of its peculiar permeability to hydrogen and to the ability to form a stable hydride (PdH_x) [2]; such hydrogen absorption causes large changes in physical properties of Pd, that are exploited for hydrogen detection in several ways. Some examples are given by resistive Pd based film sensors, Pd coated optical fibers, surface acoustic waves (SAWs), Pd based Schottky junctions, etc. [3-6]. The choice of the right technology is essentially related to the application field, depending on the considered working ranges and the required performance (in terms of selectivity, sensitivity, accuracy, reproducibility and response/recovery times). Required response time of 1s at 4%, 60 s at 1% and recovery time of 60s independent of concentration have been recently specified as target performance for H_2 safety sensors [1; 7]. Moreover, there is the need for the development of cheap sensing technologies, the required cost for target devices having been set to < 40$ per sensing node [1; 8].

The interaction between hydrogen and palladium has been extensively studied [2]. It has been demonstrated that in the case of very thin and nanostructured Pd films, characterized by some kinds of discontinuity (presence of nanopores, nanotrenches, nanowires), hydrogen absorption by Pd causes the electrical resistance to decrease: the effect is ascribed to the expansion of the Pd domains resulting in an increase of percolation [9-15]. On the contrary, the resistance increases for bulk or continuous thin films because of the increase in electron scattering due to hydrogen atoms acting as defect sites in the *fcc* lattice of palladium hydride [2; 16]. In discontinuous or nanostructured Pd films nano-scale gaps separate metal "islands"; these nano-break junctions are closed due to volume expansion upon hydrogen absorption . A phase transition, often referred to as the α phase $\rightarrow$ β phase transition [17],

occurs when the amount of adsorbed hydrogen atoms in the palladium layer exceeds the maximum H solid solubility and is responsible for change in the lattice volume up to 3,5 %.

Sensors based on such chemomechanical nano-switches approach have been described in the recent literature and showed interesting results in terms of low power consumption, speed of response, sensitivity [9; 11; 18]. Most of the cited examples used bottom-up approaches for the formation of Pd nanostructures characterized by nanogaps, e.g. discontinuous ultra-thin films obtained by physical vapor deposition (PVD) made up of island particles, Pd nanoparticles arranged into lithographically patterned channels, Pd nano- or meso-wires grown on nanostructured templates, etc. A top-down approach has been also proposed by Kiefer *et al.* milling nanotrenches into a palladium microwire with a FIB [12].

One of the drawbacks of sensors based on hydrogen induced lattice expansion of Pd is related to the mechanical stress produced on hydrogen absorption: strong adhesion at the Pd–substrate interface can hamper relaxation leading to reduced sensitivity of sensors [10]. Alternatively, poor adhesion of Pd on lower surface energy substrates cause severe stability problems related to delamination or cracking of the sensing surface and to an irreversible drift in the film electrical resistance when repeated cycles of absorption/desorption of hydrogen are imposed [17]. Many different approaches have been proposed to overcome this problem in practical devices [17-20]. Here we present an innovative approach based on the resistive properties of a microwrinkled Pd surface. By following a method recently proposed for different materials and applications, [21] the reliable formation of microwrinkles on Pd surface has been accomplished with the use of an extremely easy, fast and low-cost process. A thermoretractable pre-stressed polystyrene sheet acted as the substrate onto which a thin Pd film was deposited. The subsequent shrinkage of the substrate to 40% of its original lateral size during heating caused the formation of surface microwrinkles due to the stiffness mismatch between the Pd thin film and the shrinkable polystyrene substrate

The performance of the sensors has been studied in terms of sensitivity, response and recovery times in the range of hydrogen concentration $c_{H2} \sim 0{,}45 - 4\%$ in air and compared with similar films (on identical substrates) whose surface is not wrinkled (flat sensors) evidencing large differences in performances due to surface microstructure. The concurrent effect of both the behaviors described in literature for bulk/continuous films or discontinuous/nanogap ones (increase and decrease of resistance, respectively) has been pointed out in the sensor with microwrinkled surface, depending on hydrogen concentration. An unprecedented effect of inversion of response above a threshold value of hydrogen concentration of $c_{H2} \sim 1{,}8$ % in air has been evidenced for the microwrinkled hydrogen sensors, making it suitable the reliable detection of gas leakages just below the explosiveness limits, with competitive and low-cost sensors. The wrinkled sensors show a quite fast and reproducible response to the hydrogen exposure if compared with other resistive sensors. A complete topographical characterization (SEM, AFM, Optical microscopy) of the Pd surface of the proposed wrinkled and flat sensors is presented, along with a comparison of sensor surface topography before and after exposure to hydrogen.. The effect of thickness of the Pd film on hydrogen sensing performances as well as on surface topography and mechanical stability to hydrogen exposure has been additionally studied by comparing results with similar ones obtained for a much thinner Pd film.

2.0 MATERIALS AND METHODS

2.1 Sensors Fabrication

Hydrogen sensing experiments have been carried out simultaneously over two type of samples: 1) “Wrinkled Pd Sensor” (hereafter referred as WPS); 2) “Flat Pd Sensor” (hereafter referred as FPS. Geometry of the two different samples has been properly set up in order to perform hydrogen sensing measurements over Pd stripes of the same final size.

Wrinkled Pd Sensor (WPS)

Micro-wrinkled palladium thin films were fabricated as rectangular-shaped stripes through deposition of palladium on thermo-retractable and pre-stressed polystyrene sheet, commercially available with the name of Polyshrink™ (Lucky Squirrel, US). A peculiar characteristic of this material lies in its ability, when properly heated, to irreversibly shrink to 40% of its original size along its surface while

expanding its thickness. Translucent Polyshrink™ foils were cut in 34 mm x 9 mm sheets and then used as substrate for the Pd deposition using aluminium physical mask with a 30 mm x 5 mm hole

The Pd deposition on the masked samples has been performed by a DCC 150 DC/AC magnetron sputtering system (Sistec, Italy) operating at a constant pressure of 1 Pa, equipped with a 101.6 mm diameter Pd target. Deposition has been performed for 120s with 90 W of sputtering power (WPS_{120} sample). Pure Argon was used as sputtering gas. Additional samples with thinner Pd film have been obtained by using a deposition time of 30s at same sputtering power (WPS_{30} sample). After the Pd deposition, the specimens were heated in oven at 170°C for ~6 minutes, thus obtaining 13.6 mm x 3.6 mm shrunk samples, with a 12 mm x 2 mm wrinkled Pd surface.

Flat Pd Sensor (FPS)

Fabrication process of Flat Pd Sensors is the same of the wrinkled ones, except for the final step of shrinkage upon heating, that was avoided. In order to keep the same final size of wrinkled specimens, 13.6 mm x 3.6 mm Polyshrink™ sheets have been used as substrate and aluminium masks with a 12 mm x 2 mm hole Along with FPS_{120} samples, (sputter deposition time 120sFPS_{30} samples were prepared (deposition time 30 s).).

Control Pd Film (CPF)

Control Pd Films have been fabricated by sputtering the metal on a cleaned standard glass for microscopy simultaneously with Wrinkled and Flat Sensors, in order to maintain the same conditions (obtaining CPF_{120} and CPF_{30} samples, with 120 and 30 s of sputtering, respectively).

2.2 Sensors Surface Characterization

Images of WPS and FPS samples were taken by using an Hirox KH7700 digital microscope (Hirox Co Ltd., Tokyo, Japan), equipped with a MX(G)-10C zoom lens and OL-700II objective lens. Microscopic images of WPS and FPS samples were acquired with an EVO®MA10 Scanning Electron Microscope (SEM) (Zeiss; Germany) using acceleration voltage of 9-10 kV and aperture size of 30 μm. Thickness and topography of the CPF samples were evaluated in air and at room temperature with an Atomic Force Microscope (AFM) of Veeco Innova Scanning Probe Microscope (Veeco Instruments Inc., Santa Barbara, CA) operating in tapping mode, using a RTESPA Al coated silicon probe (Veeco Instruments Inc.). CPF samples were scratched with a needle and surface was scanned across the scratched edge over a 20 μm × 20 μm area, recording 512 × 512 samples, allowing for thickness measurement. The resulting scan data were elaborated using Gwyddion SPM analysis tool (free download from http://gwyddion.net). Scan data were leveled with a facet level tool to remove sample tilt, and then the sample profile was extracted in a direction perpendicular to the scratch edge. Height data were averaged on rows, and the thickness was evaluated as the difference between horizontal lines fitting glass and the Pd film surface profiles.

2.3 Hydrogen Sensing Measurement Setup

The sensitivity of the Pd films to hydrogen has been characterized by measuring the electrical resistance while undergoing the samples to a controlled air/hydrogen mixture (generated with *ad hoc* test system, by using an air pump and a current driven electrolyzer), at room temperature. Electrical contacts on Pd films were made by means of CircuitWorks® Conductive Epoxy CW2400 (ITW Chemtronics, US). Electrical resistance measurements as function of time for different hydrogen concentrations were carried out simultaneously over the WPS and FPS samples, inside a suitable test chamber. The test system is schematically reported in Figure 1.

The fluidic part of the test system included an Electrolyzer 65 (h-Tech, Germany), a trap for collecting condensing water, a 3-way valve, a test chamber containing the specimens, a AWM3300V microbridge mass airflow sensor (Honeywell, US), a manual flow regulator and a N022AT.18 membrane air pump (KNF, Germany). The circuit worked in aspiration in order to reduce the pollution of specimens. A pressure buffer (one liter empty vessel) has been coupled with the manual regulator in order to suppress the flow fluctuation induced by the membrane pump. All the components were connected by silicon tubes.

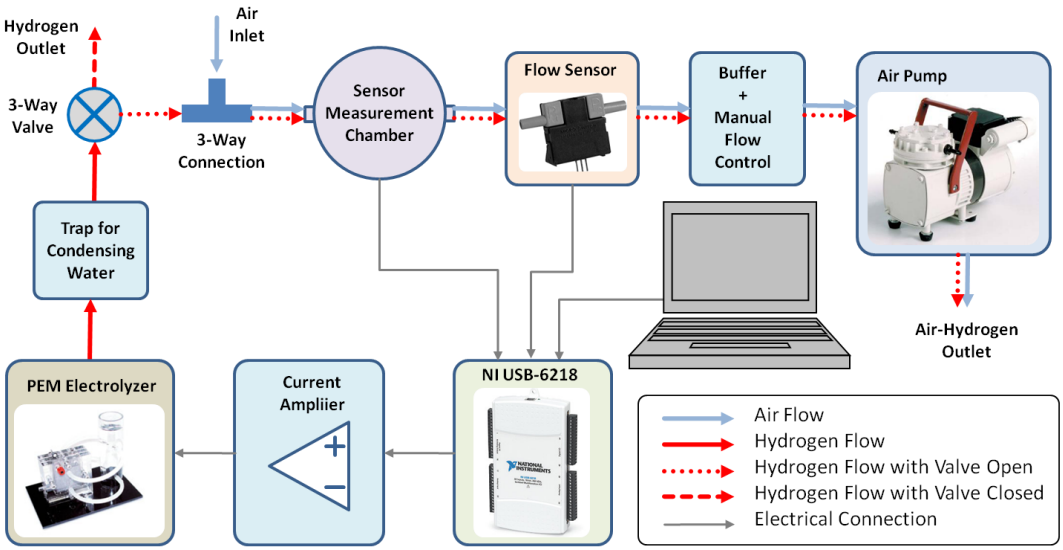

Figure 1. Schematic view of testing setup for hydrogen sensing measurement.

A NI USB-6218 data acquisition board (National Instruments, US) and a dedicate software was used to control the hydrogen production, and to acquire the experimental data, including resistance of sensors and flowmeter output. A dedicated current amplifier based on OPA549 integrated operational amplifier (Texas Instruments, US), controlled by the NI USB-6218 card, provided the necessary current (up to 5A) to the electrolyzer.

All sensors measurements have been carried out maintaining a nominal air flow rate of 1 l/min. The complete set of measurements included eight different hydrogen concentrations (from 0,45%$_{vol}$ to 4 %$_{vol}$ with ~ 0,5% incremental steps). At least four On-Off cycles (hydrogen valve Open/Closed) have been recorded for each concentration. Variable time for On-Off cycles has been used on the basis of the sensor response time. The measured signal of resistance R vs. time has been converted to $\Delta R/R_0$ (%) (resistance change magnitude), using the following formula:

$$\Delta R/R_0 = 100 \times (R - R_0)/R_0 \quad (1),$$

where R is the measured sensor resistance, while R_0 is the measured value of R in the initial state, i.e. in a H_2 free environment. In order to follow the trend of sensor sensitivity against increasing hydrogen concentration and to compare the different behaviors of the two kinds of sensors, we calculated the sensitivity (S) both for response (S_{Resp}) and recovery (S_{Rec}) in each cycle of hydrogen/air exposure for each studied hydrogen concentration, defined as:

$$S_{Resp} = 100 \times (R_{H2on} - R_{H2off})/R_0 \quad (2),$$

$$S_{Rec} = 100 \times (R_{H2off} - R_{H2on})/R_0 \quad (3).$$

3.0 RESULTS AND DISCUSSION

3.1 Thickness and Surface Topography Characterization

Thickness *t* of the Pd thin films has been estimated on the CPF samples. AFM images for Pd films with different deposition times are shown in Figure 2. Thickness of the deposited film is t_{30} = 30 ± 6 nm and t_{120} = 105 ± 10 nm for CPF_{30} and CPF_{120} samples, respectively.

The creation of the microwrinkled Pd surface of sensors has been obtained by shrinking the thermo-retractable substrate, Such unconventional method was recently proposed by the group of Prof. M. Khine that described the tunable formation of biaxial or uniaxial micro and nanowrinkles on the surface of Au or Ag thin films deposited onto thermo-retractable polystyrene [21]. Wrinkles arise because of compressive strain acting on the thin metal layer during shrinkage of substrate [22].

SEM pictures of the wrinkled Pd surfaces of WPS sensors shown in Figure 3.a and b, clearly depict the micro-structured surface characterized by uniform isotropic micro and nano-wrinkles over the whole area of sensors (24 mm^2). Wavelength and amplitude of such wrinkles are dependent on

thickness of the metal layer although a broad wavelengths distribution can be evaluated with the use of 2D FFT on SEM images (not shown here).

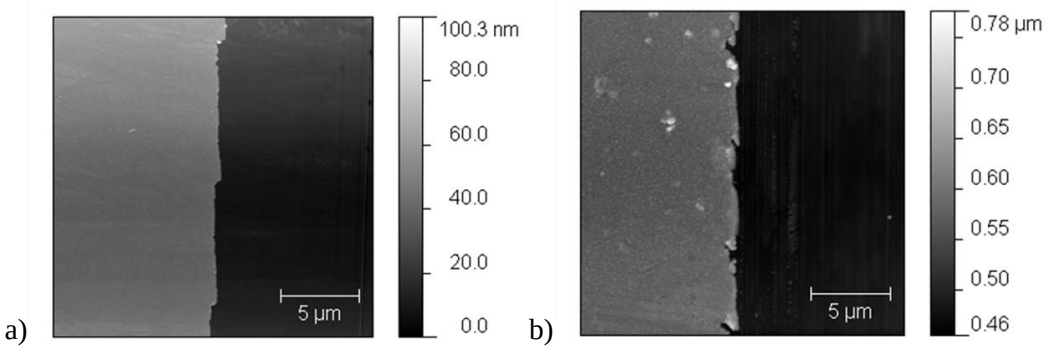

Figure 2. AFM scansions of the scratched surface of palladium on CPF samples on glass: a) CPF30 sample; b) CPF120 sample. Thickness of films was obtained by measuring the height profile of the edge between the Pd film (moderately rough surface) and the scratched domain (flat).

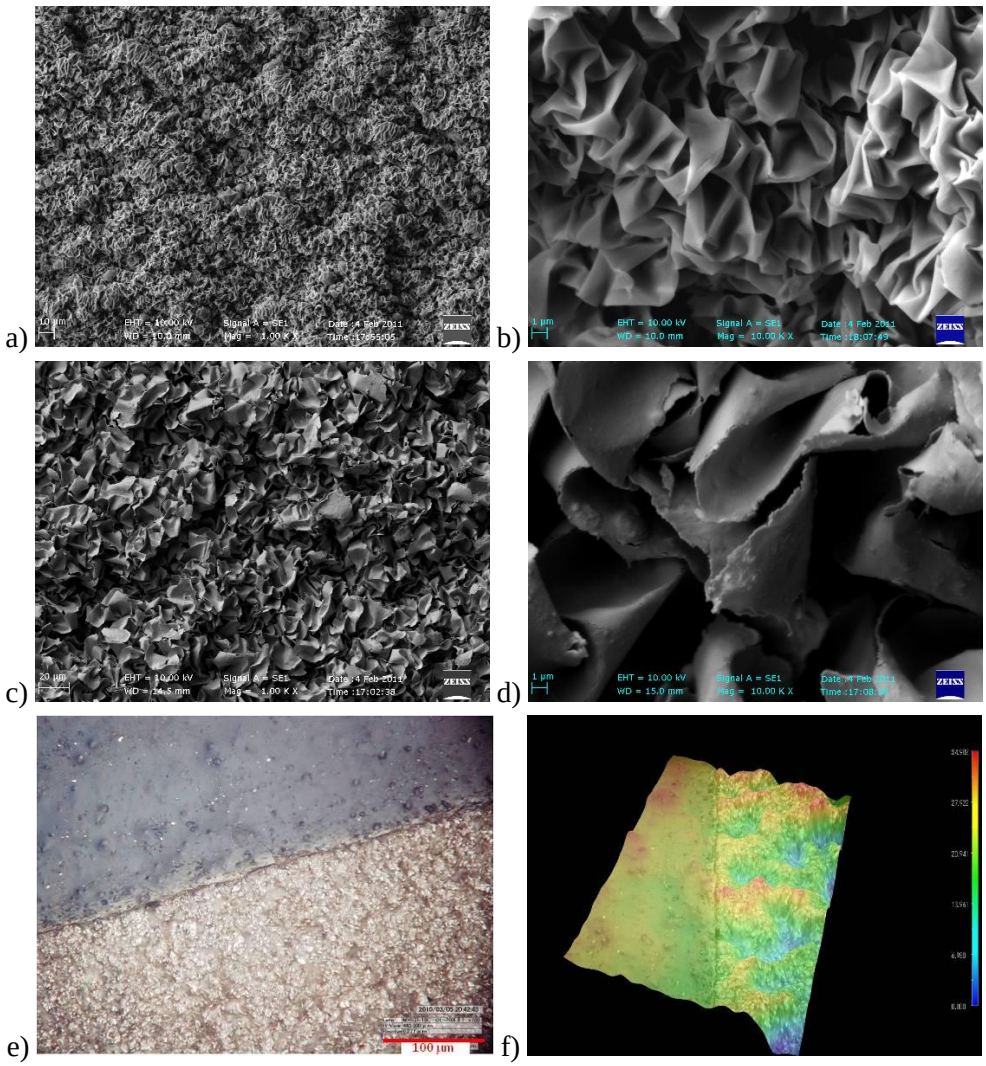

Figure 3. SEM micrographs at two different magnifications (1 KX, 10 KX) of the Pd surface of WPS_{30} (a,b) and and WPS_{120} (c,d) samples. e) Digital optical microscope image of a border area of the WPS_{120} sample comprising a wrinkled Pd surface (bottom) and masked PS surface (up); f) 3D digital reconstruction of the same surface obtained through focus scansion with a Hirox digital microscope.

Difference in wrinkles wavelengths and shape can be qualitatively appreciated by comparing Figure 3.a,b and c,d depicting respectively the surface of WPS_{30} and WPS_{120} samples. Figure 3.e,f

show the uniform formation of micro-wrinkles on the whole Pd surface of the sensor and the hierarchical generation of wrinkles (coexistence of wrinkles at various wavelengths and amplitudes superimposing each other). WPS sensor surface is characterized by the continuous alternation of peaks and valleys whose heights vary within some tens of micrometers (Figure 3.f, right part), differently from the almost flat bare polystyrene (left part). A final and important remark on surface topography is related to the integration of Pd wrinkled film with the supporting PS substrate. Indeed, the heating process that induce shrinking of the retractable substrate and buckling of the not-retractable metal is performed at T = 170°C, above glass transition temperature of PS ($T_g \approx 95°C$). At the processing temperature the PS substrate is therefore soft enough to cause the integration of the buckling metal film. The formed wrinkles are very strong and durable, and the metal to substrate adhesion is improved compared to flat samples. We have empirically tested the good adhesion and stability of wrinkles: peeling off or partial removal of Pd film is avoided even when scratching the surface. The surface can also bear a cleaning in an ultrasonic bath for several minutes.

Figure 4 shows SEM micrographs of the surface of FPS samples, in which Pd has been deposited onto substrate without performing the heat-shrink process. The bumps and circular features at the surface are ascribable to the pristine PS surface onto which the Pd film has been deposited. No relevant differences have been outlined among the Pd films with different thicknesses.

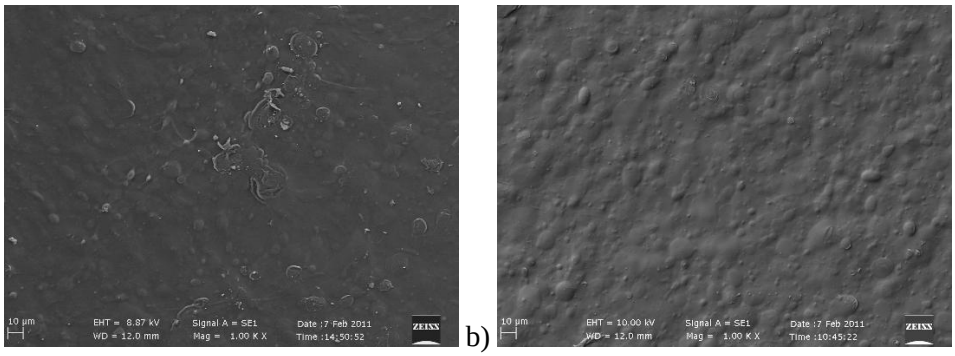

Figure 4. SEM micrographs (magnification 1 KX) of the Pd surface of FPS_{30} (a) and FPS_{120} (b) samples.

3.2 Hydrogen Sensing: flat and wrinkled sensors

The results of hydrogen sensing experiments performed on FPS_{120} and WPS_{120} samples are reported in Figure 5.a and b respectively. The two kinds of studied sensors show a very different behavior upon hydrogen exposure. Resistance of FPS_{120} decreases upon hydrogen exposure for each studied concentration, i.e. $c_{H2} = 0{,}45 – 4\%$ in air, (Figure 5.a). On the other hand, resistance of WPS_{120} sample exhibits a similar decrease -although lower in magnitude- upon hydrogen exposure at low hydrogen concentration regime (0,45 - 1,3% H_2 in air). Around 1,5 - 1,8 % concentration the net resistance change become negligible, while for $c_{H2} > 1{,}8$ % up to the maximum studied concentration value the sensor resistance increases upon hydrogen exposure.

Figure 6 shows the trends of response sensitivity S_{Resp} as a function of hydrogen concentration for the flat and the wrinkled sensors. Sensitivity in response only is shown for clarity purpose and because nearly identical and opposite response and recovery sensitivity have been measured as reported in Figure 5 and Figure 7. It is important to notice that some drift (≈ 5% of absolute resistance value), relative to a hysteretic behavior (due to irreversible changes occurring at Pd surface during hydrogen absorption) has been recorded for flat sensors only during the first cycles of hydrogen absorption/desorption. Such hysteresis behavior, well described in recent literature [17], is much less relevant in wrinkled sensors (see for comparison Figure 5.a and b). The monotonous decrease observed for FPS_{120} sample with increasing hydrogen concentration is ascribable to a percolation enhancement effect; Pd lattice expansion due to H_2 absorption causes gaps of the thin inhomogeneous Pd surface to be filled so enhancing the conductive pathways with the overall effect of reducing electrical resistance. Such behavior, already described for discontinuous Pd film characterized by the presence of nano-gaps [9-15], takes place in flat sensors because of the discontinuous nature of the as deposited Pd films onto the polymer substrate, made up of individual grains. No saturation of such

effect is evidenced in the specified H_2 concentration range although some evidence of change in the trend slope are emerging around 2,5% H_2 concentration after a plateau region in the 1% - 2% range. This effect could be rationalized in the frame of $\alpha \rightarrow \beta$ phase transition occurring in Palladium hydride at such hydrogen concentration level [17].

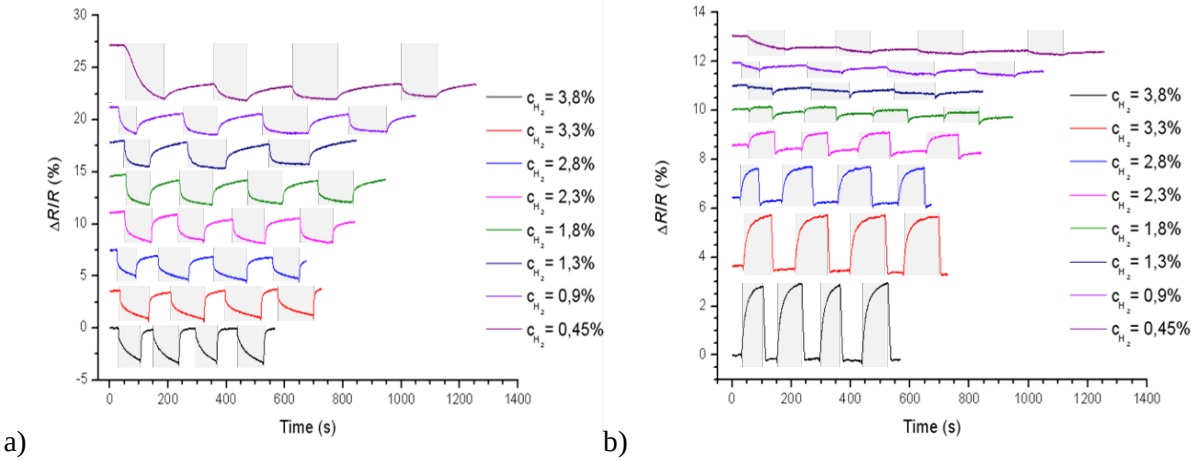

a) b)

Figure 5. Summary of hydrogen sensing experiments on FPS_{120} (a) and WPS_{120} (b) samples. Each line represents the resistance change magnitude $\Delta R/R_0$ (%) measured in a single experiment in which 4 consecutive cycles of exposure to hydrogen (gray filled areas corresponds to hydrogen valve Open) have been performed at different hydrogen concentrations. Lines are shifted vertically for clarity.

Concerning WPS_{120} sample, the trend of sensitivity against hydrogen concentration shows a very different behavior compared to the flat one. At low hydrogen concentration, sensor resistance decreases upon hydrogen exposure, so negative sensitivity values are found, slightly decreasing down to S_{Resp} = -0,32 % for c_{H2} = 0,9 %, a poorer value with respect to that recorded for flat sensors S_{Resp} = -2,20 %). For c_{H2} > 1 %, the trend is inverted: S_{Resp} increases with hydrogen concentration, it reaches positive values for c_{H2} > 1,5 % and eventually increases steadily up to S_{Resp} = 3,1 % for c_{H2} = 4 %. In summary, the sensor, crossing null sensitivity at c_{H2} = 1,5 %, shows poor negative sensitivity at low hydrogen concentration and improved positive sensitivity at higher concentration, near to Lower Explosive Limit (LEL) of hydrogen in air.

In order to get more insight in such a complex behavior, it is instructive to look at sensitivity measurements reported in Figure 5.b. In the case of measurements performed around the threshold value c_{H2} = 1,5 % (activation threshold, c_{Act}), the coexistence of two counteracting effects is evident. The first one, also active in FPS_{120} sensor, is responsible for lowering resistance upon hydrogen exposure, and starts immediately after H_2 is turned on. The second one, superimposing to the first and gradually compensating its effect after some time, tends to improve resistance. At threshold value, these counteracting effects are exactly balancing each other, so resulting in null net sensitivity, once stability is reached. The competition of both effects at higher H_2 concentration exposure, although less evident, is still recognizable in the recorded signals reported in Figure 5: resistance (and hence sensitivity) quickly drops when hydrogen is turned on; this drop is then compensated and overwhelmed by a large increase in resistance.

These unexpected results can be rationalized by taking into account the peculiar topography of the wrinkled sensors. The marked micro-wrinkles, while improving the active surface area of the sensor with respect to flat ones, create new and shorter conductive pathways between points in the surface that would be very far apart if in a flat surface. The wrinkles can come in contact with neighboring wrinkles as it is shown in SEM pictures reported in Figure 3. In this way, a sort of micro-structured "skin" is formed whose thickness (several micrometers) is larger than the thickness of Pd layer (105 nm) and comparable to wrinkles amplitude. Such evidence is also confirmed by the value of electrical resistance measured before hydrogen exposure that is in the order of R = 20 - 30 Ω for WPS_{120}, to be compared with R = 500 - 600 Ω for FPS_{120}. Moreover, the expansion of Pd layer due to hydrogen absorption causes the closing of more and more gaps between adjacent wrinkles and the reversible establishment of a "bulk-like" Pd surface. For this reason, in a single experiment increasing

hydrogen content initially causes a decrease in resistance up to a concentration threshold value (activation threshold), corresponding to maximum obtainable percolation enhancement; above this threshold further hydrogen adsorption causes an increase in resistance of the sensor, as in continuous Pd films. Very interestingly this behavior is reversible: restoring the air environment causes a complete recovery of the original resistance of the sensor.

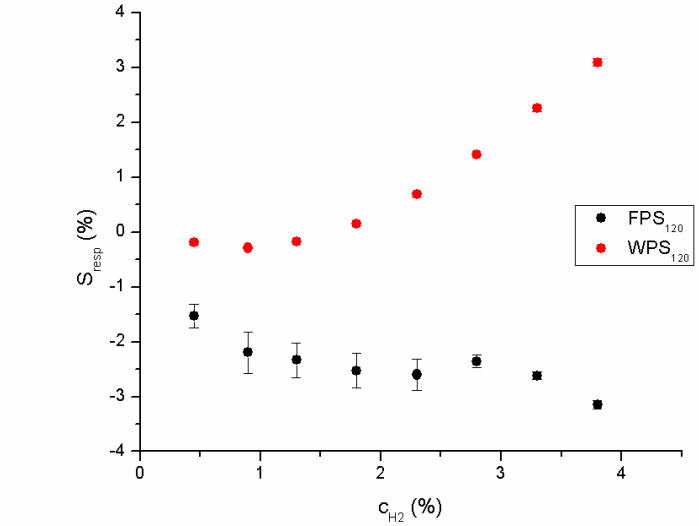

Figure 6. Response sensitivity (S_{Resp}) as obtained for FPS_{120} (black circles) and WPS_{120} (red circles) samples as a function of hydrogen concentration c_{H2}.

3.3 Pd-layer Thickness Effect on Hydrogen Sensing Behavior

In order to get more insight in the mechanism governing the behavior observed in FPS_{120} and WPS_{120} samples, we performed same hydrogen sensing experiments on similar sensors with smaller Pd film thickness (FPS_{30} and WPS_{30}). Indeed, the peculiar topography is largely related to the thickness of the Pd layer (see SEM pictures in Figure 3). In Figure 7 we report the compared behavior of sensors with different Pd-layer thickness, for both response and recovery steps upon hydrogen exposure. Trends for the two kinds of sensors are very similar, particularly for the wrinkled sensors (Figure 7.b), despite the large differences observed in topography. Moreover the response/recovery sensitivity is almost symmetrical (no significant drift in resistance) for all the samples.

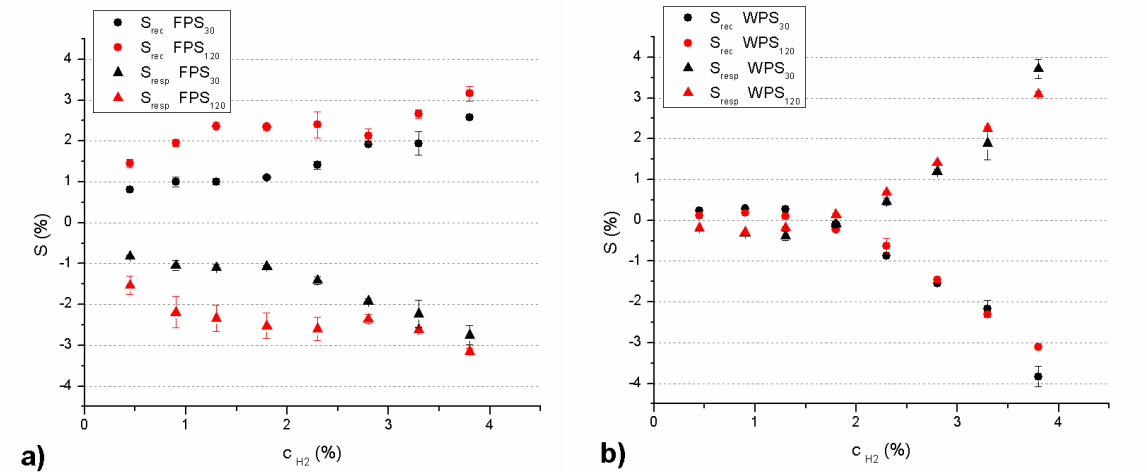

Figure 7. Sensitivity in response (triangles) and recovery (circles) upon hydrogen exposure as a function of hydrogen concentration; comparison of wrinkled sensors (a) (WPS_{30} black, WPS_{120} red) and flat sensors (b) (FPS_{30} black, FPS_{120} red).

As regards FPS_{30} and FPS_{120} samples (Figure 7.a) the sensitivity has a little improvement with increasing thickness of Pd layer and the difference in sensors performance is more pronounced in the 1% - 2,5% range. The change in the trend slope for FPS_{30} is shifted to lower hydrogen concentration,

i.e. at $c_{H2} \sim 2\%$, probably due to lower mechanical constraints occurring in thinner Pd films acting against the lattice expansion induced by phase transition [17].

Concerning WPS sensors, Figure 7.b, the reported trends for both thicknesses are almost identical, with some minor differences: the most important one is related to what we have called the "activation threshold". By interpolating the obtained trends (data not shown here) and carefully looking at the null sensitivity crossing for both trends it is possible to evaluate two different activation threshold c_{Act} for the two thicknesses, i.e. $c_{Act} \sim 1{,}5\%$ for WPS_{120} sample while $c_{Act} \sim 1{,}8\%$ for WPS_{30} sample. Such a change is ascribable to the differences in surface topography discussed in Section 3.1 and can possibly open the way to tailoring of sensors in terms of their activation threshold by fine tuning of micro-wrinkling. This fine tuning, already demonstrated in the case of Au or Ag with varying thickness of metal layer onto thermo-retractable substrate [21], will permit to select the right activation threshold depending on the required performances of hydrogen sensors.

3.4 Effects of Hydrogen Exposure on Sensors Topography

The stability of sensors has been evaluated by inspecting their surface topography with SEM before and after exposure to hydrogen. Concerning flat sensors, Figure 8, micro-fractures appear on the surface of FPS120 due to lattice expansion/contraction during repeated H_2 adsorption/desorption cycles. The micro-cracks seem to be wider and denser in correspondence of bumps and irregular features characterizing the pristine surface of Polyshrink, as seen in Section 3.1. No cracking appear in FPS30 samples with thinner Pd-layer: in this case no change is evidenced in SEM micrographs of surfaces before and after hydrogen exposure, Figure 8.a and b). A similar suppression of mechanical deformation occurring in films with comparable thickness but on different substrates has been recently described. [17] Authors claimed for a thickness-dependent effect of clamping: the tensile stiffness for a bi-layer (laminate sample) is inversely proportional to thickness. [6] Therefore, the tensile strength induced in the Pd layer decreases as the thickness of Pd layer is reduced. Additionally, due to better flexibility with respect to other substrates, Polyshrink allows the expansion/contraction of Pd upon cycled hydrogen loading, while maintaining good adhesion properties, as described for polyimide substrates [14]. Concerning wrinkled sensors topography, no fractures are evidenced on WPS_{30} sample surface after hydrogen exposure (Figure 9.a and b). Wrinkles density seems to be increased after hydrogen exposure: the strain induced by lattice expansion during hydrogen sensing experiments causes new wrinkles to appear, without compromising the performance and stability of the sensor and the adhesion to substrate. Probably, due to previously cited clamping effect, the thin Pd layer retains a certain plasticity that permit the buckling without the formation of cracks. On the other hand, the already fractured surface of pristine WPS_{120} sample seems to be not apparently affected by hydrogen exposure (Figure 9.c and d). Probably the already fractured and peeled-off Pd surface is more effective in adsorbing/relaxing stress induced by lattice expansion.

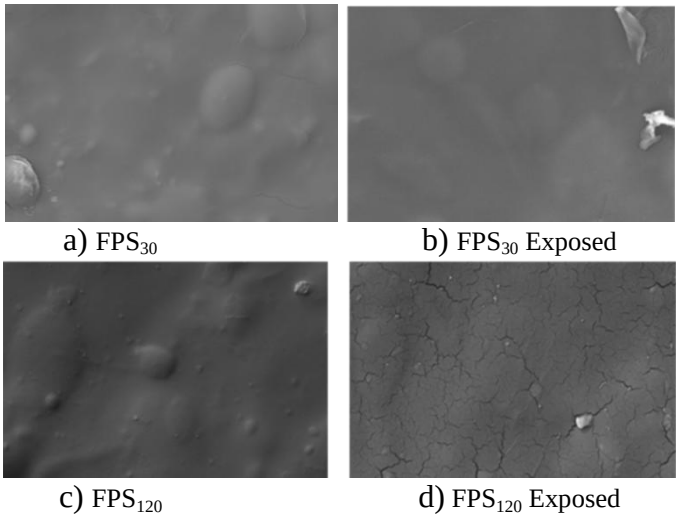

a) FPS_{30} b) FPS_{30} Exposed

c) FPS_{120} d) FPS_{120} Exposed

Figure 8. Effects of hydrogen exposure on flat sensors. SEM micrographs (magnifications 10 KX) of FPS_{30} (a,b) FPS_{120} (c,d) before exposure to hydrogen (a,c) and after exposure to hydrogen (b,d).

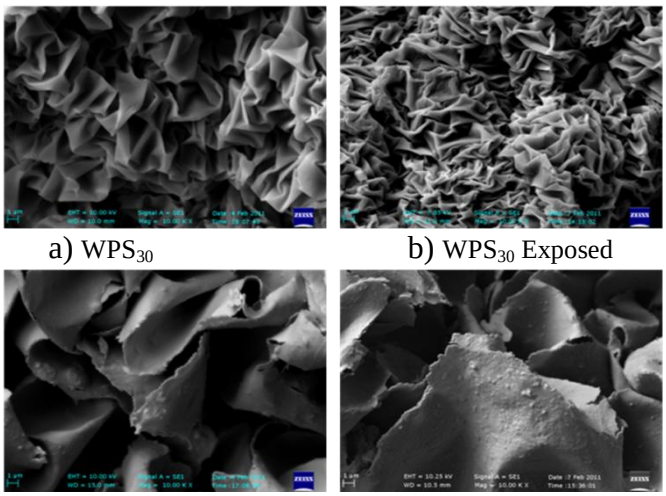

a) WPS_{30} b) WPS_{30} Exposed

c) WPS_{120} d) WPS_{120} Exposed

Figure 9. Effects of hydrogen exposure on wrinkled sensors. SEM micrographs of WPS_{30} (a,b) WPS_{120} (c,d) before exposure to hydrogen (a,c) and after exposure to hydrogen (b,d).

3.5 Hydrogen Sensing Response and Recovery Times

Speed of response/recovery of H_2 safety sensors is an important parameter as fast detection of gas leakages represents an essential requirement, e.g. for the use of hydrogen as a fuel in automotive applications. We calculated the rise time and fall time of the recorded signals of electrical resistance during exposure respectively to hydrogen/air or air environment. The response time, τ_{resp}, (alternatively, recovery time, τ_{rec}) has been defined as the time required for the sensor to reach 90% of the overall resistance change on hydrogen exposure (alternatively, on air exposure). Figure 10.a reports the data of response time τ_{resp} obtained at different hydrogen concentrations in sensing experiments. The τ_{resp} is almost constant for FPS in the studied hydrogen concentration range. The values of τ_{resp} strongly depend on Pd-film thickness, being e.g. τ_{resp} = 227s in FPS_{30} and τ_{resp} = 47s in FPS_{120} at c_{H2} = 2,3 %. On the other hand, samples the overall trend of τ_{resp} for WPS samples is more complex than in FPS, i.e. a discontinous trend as a function of hydrogen concentration is observed, similarly to sensitivity results. As a general feature, reduced response times have been measured for WPS_{120} sensors with respect to WPS_{30}:in the overall studied range WPS_{120} sensors showed τ_{resp} < 50 s.

More interesting results have been obtained for recovery times and are reported in Figure 10.b.Both FPS_{30} and FPS_{120} have regular trends of monotonous, continuous decrease in τ_{rec} with increasing hydrogen concentration . The two trends are almost parallel in the 0,45% < c_{H2} < 4% range with τ_{rec} varying from 185 s to 105 s for FPS_{30}, and from 130 s to 20 s for FPS_{120}. Analogously to response time, WPS samples show a discontinous trend of recovery time as a function of hydrogen concentration . Indeed, while showing similar values of recovery time to FPS samples at the lower limit of studied hydrogen concentration, τ_{rec} of WPS abruptly drops to very small values in correspondence to the activation threshold. Recovery time as small as τ_{rec} = 1,5 s has been recorded in WPS_{120} at c_{H2} = 1,8%. The τ_{rec} increases with increasing c_{H2} above the activation threshold and eventually reaches the values observed for flat sensors at c_{H2} = 4%. WPS_{120} samples show faster recovery time with respect to WPS_{30}, : in the "activated" range τ_{rec} varies from 1,5 s to 8 s in the case of WPS_{120}, and from 16 s to 90 s in the case of WPS_{30}.

What is important to notice is that the wrinkled sensors above the activation threshold are very fast, similarly to nanostructured ones, while having an opposite behavior in terms of sensitivity (sign of the resistance change upon hydrogen loading). In the case of sensitivity, indeed, their behavior is more similar to bulk or thicker Pd films. Notably, at least for thicker wrinkled Pd films, the observed recovery time is suitable for technological application, the required performance having been fixed to τ_{rec} = 60 s independent of hydrogen concentration [1; 8].

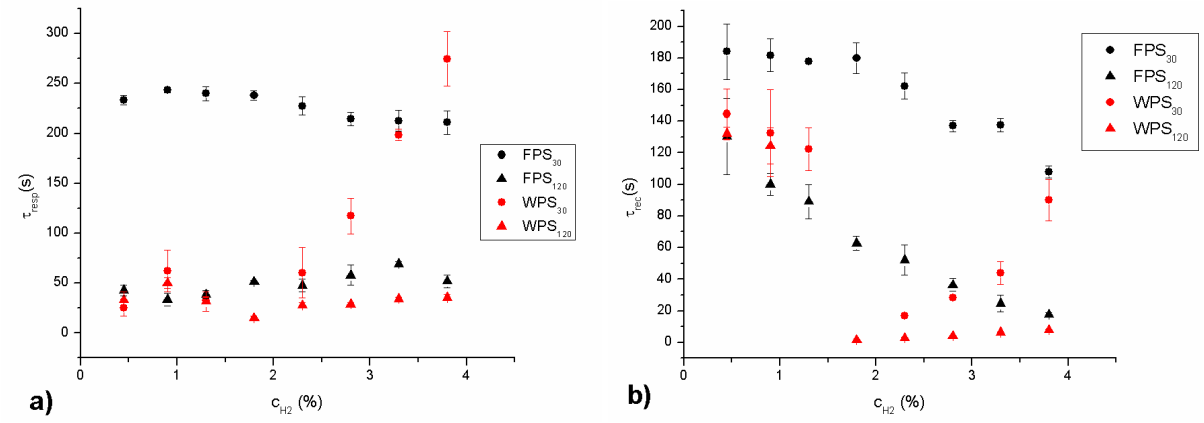

Figure 10. Characteristic response time (τ_{resp}, a) and recovery time (τ_{rec}, b) for the studied sensors as a function of hydrogen concentration employed in sensing experiments. Comparison between flat samples (black symbols; FPS_{30} circle, FPS_{120} triangle) and wrinkled samples (red symbols; WPS_{30} circle, WPS_{120} triangle).

4. CONCLUSIONS

In this paper we reported the fabrication and characterization of a novel hydrogen sensor using a fast and cheap technology. The development of a micro-wrinkled palladium surface obtained through sputtering deposition onto a thermo-retractable polystyrene substrate was described. The proposed sensors were tested in a suitable test set-up in the range of 0.45 - 4% hydrogen concentration in air, that is relevant for the proposed safety application. Surface topography and its effects in determining sensor performances were also evaluated as well as the surface stability to hydrogen exposure.

One of the major finding of this study is related to the switching response that the wrinkled sensors show. The sensitivity of these sensors switches from poor negative value to large positive one when the hydrogen concentrations overcome a certain threshold and approach Lower Explosive Limit of hydrogen in air. The activation threshold, related to the size and shapes of microwrinkles characterizing sensor surface, can be tuned by changing the thickness of palladium film. A rationalisation of the mechanism governing the observed behaviour was also provided, on the basis of the well known opposite effects of percolation enhancement and resistivity increase, acting in palladium hydride upon hydrogen exposure. Additionally, the wrinkled sensors show a very fast recovery time, respect to comparable Pd resistive sensors, in the hydrogen concentration range of interest. A comprehensive comparison of sensor performances in terms of sensitivity and of response/recovery time has been provided for micro-wrinkled samples with respect to flat ones.

The peculiar performances of micro-wrinkled samples, in addition to the cheapness and the stability, make the proposed sensor a very interesting candidate for applications in the automotive field. Indeed, above the activation threshold, the sensitivity of the sensor seems to be mostly uninfluenced by thickness of Pd layer, and then reproducible behavior can be foreseen also without strict fabrication requirement.

ACKNOWLEDGMENTS

This work was partially supported by the project "H_2 Filiera Idrogeno" funded by "Regione Toscana". Mr. Carlo Filippeschi and Miss Silvia Taccola are acknowledged for their support in performing DC magnetron sputtering of Pd films and AFM scansions of sensors surface, respectively.

REFERENCES

1. Buttner, W.J., Post, M.B., Burgess, R. and Rivkin, C., An overview of hydrogen safety sensors and requirements, *International Journal of Hydrogen Energy*, **36**, No. 3, 2011, pp. 2462-2470.
2. Lewis, F.A., Palladium Hydrogen System,1967. Academic Press, London, New York.

3. Wolfe, D.B., Love, J.C., Paul, K.E., Chabinyc, M.L. and Whitesides, G.M., Fabrication of palladium-based microelectronic devices by microcontact printing, *Applied Physics Letters*, **80**, No. 12, 2002, pp. 2222-2224.
4. Jakubik, W.P., Urbanczyk, M.W., Kochowski, S. and Bodzenta, J., Bilayer structure for hydrogen detection in a surface acoustic wave sensor system, *Sensors and Actuators B: Chemical*, **82**, No. 2-3, 2002, pp. 265-271.
5. Tobiska, P., Hugon, O., Trouillet, A. and Gagnaire, H., An integrated optic hydrogen sensor based on SPR on palladium, *Sensors and Actuators B: Chemical*, **74**, No. 1-3, 2001, pp. 168-172.
6. Lundstrom, I., Shivaraman, S., Svensson, C. and Lundkvist, L., A hydrogen - sensitive MOS field - effect transistor, *Applied Physics Letters*, **26**, No. 2, 1975, pp. 55-57.
7. Rivkin, C., Blake, C., Burgess, R., Buttner, W.J. and Post, M.B., A national set of hydrogen codes and standards for the United States, *International Journal of Hydrogen Energy*, **36**, No. 3, 2011, pp. 2736-2741.
8. Yang, F., Taggart, D.K. and Penner, R.M., Joule Heating a Palladium Nanowire Sensor for Accelerated Response and Recovery to Hydrogen Gas, *Small*, **6**, No. 13, 2010, pp. 1422-1429.
9. Favier, F., Walter, E.C., Zach, M.P., Benter, T. and Penner, R.M., Hydrogen Sensors and Switches from Electrodeposited Palladium Mesowire Arrays, *Science*, **293**, No. 5538, 2001, pp. 2227-2231.
10. Dankert, O. and Pundt, A., Hydrogen-induced percolation in discontinuous films, *Applied Physics Letters*, **81**, No. 9, 2002, pp. 1618-1620.
11. Luongo, K., Sine, A. and Bhansali, S., Development of a highly sensitive porous Si-based hydrogen sensor using Pd nano-structures, *Sensors and Actuators B: Chemical*, **111-112**, No. 2005, pp. 125-129.
12. Kiefer, T. and et al., A single nanotrench in a palladium microwire for hydrogen detection, *Nanotechnology*, **19**, No. 12, 2008, pp. 125502.
13. Kiefer, T., Villanueva, L.G., Fargier, F., Favier, F. and Brugger, J., The transition in hydrogen sensing behavior in noncontinuous palladium films, *Applied Physics Letters*, **97**, No. 12, 2010, pp. 121911-121913.
14. Kiefer, T., Villanueva, L.G., Fargier, F., Favier, F. and Brugger, J., Fast and robust hydrogen sensors based on discontinuous palladium films on polyimide, fabricated on a wafer scale, *Nanotechnology*, **21**, No. 50, 2010, pp. 505501.
15. Sun, Y. and Wang, H.H., High-Performance, Flexible Hydrogen Sensors That Use Carbon Nanotubes Decorated with Palladium Nanoparticles, *Advanced Materials*, **19**, No. 19, 2007, pp. 2818-2823.
16. RaviPrakash, J., McDaniel, A.H., Horn, M., Pilione, L., Sunal, P., Messier, R., McGrath, R.T. and Schweighardt, F.K., Hydrogen sensors: Role of palladium thin film morphology, *Sensors and Actuators B: Chemical*, **120**, No. 2, 2007, pp. 439-446.
17. Lee, E., Lee, J.M., Koo, J.H., Lee, W. and Lee, T., Hysteresis behavior of electrical resistance in Pd thin films during the process of absorption and desorption of hydrogen gas, *International Journal of Hydrogen Energy*, **35**, No. 13, 2010, pp. 6984-6991.
18. Xu, T., Zach, M.P., Xiao, Z.L., Rosenmann, D., Welp, U., Kwok, W.K. and Crabtree, G.W., Self-assembled monolayer-enhanced hydrogen sensing with ultrathin palladium films, *Applied Physics Letters*, **86**, No. 20, 2005, pp. 203104-203103.
19. Hughes, R.C. and Schubert, W.K., Thin films of Pd/Ni alloys for detection of high hydrogen concentrations, *Journal of Applied Physics*, **71**, No. 1, 1992, pp. 542-544.
20. Fedtke, P., Wienecke, M., Bunescu, M.-C., Pietrzak, M., Deistung, K. and Borchardt, E., Hydrogen sensor based on optical and electrical switching, *Sensors and Actuators B: Chemical*, **100**, No. 1-2, 2004, pp. 151-157.
21. Fu, C.-C., Grimes, A., Long, M., Ferri, C.G.L., Rich, B.D., Ghosh, S., Ghosh, S., Lee, L.P., Gopinathan, A. and Khine, M., Tunable Nanowrinkles on Shape Memory Polymer Sheets, *Advanced Materials*, **21**, No. 44, 2009, pp. 4472-4476.
22. Genzer, J. and Groenewold, J., Soft matter with hard skin: From skin wrinkles to templating and material characterization, *Soft Matter*, **2**, No. 4, 2006, pp. 310-323.